

A Data-driven Spatial Approach to Characterize Flood Hazard

Rubayet Bin Mostafiz^{1,2†*}, Md. Adilur Rahim^{3†}, Carol J. Friedland⁴, Robert V. Rohli^{1,2}, Nazla Bushra¹, Fatemeh Orooji⁵

¹Department of Oceanography & Coastal Sciences, College of the Coast & Environment, Louisiana State University, Baton Rouge, LA, United States

²Coastal Studies Institute, Louisiana State University, Baton Rouge, LA, United States

³Engineering Science Program, Louisiana State University, Baton Rouge, LA, United States

⁴LaHouse Resource Center, Department of Biological and Agricultural Engineering, Louisiana State University Agricultural Center, Baton Rouge, LA, USA

⁵Architectural Sciences, Western Kentucky University, Bowling Green, KY, United States

* Correspondence:

Rubayet Bin Mostafiz
rbinmo1@lsu.edu

Keywords: annual exceedance probability (AEP), Gumbel extreme value distribution, spatial interpolation techniques, Special Flood Hazard Area (SFHA), Federal Emergency Management Agency (FEMA), flood risk, shaded X Zone, unshaded X Zone

Abstract

The United States Federal Emergency Management Agency (FEMA) provides model-output localized flood grids that are useful in characterizing flood hazards for properties located in the Special Flood Hazard Area (SFHA — areas expected to experience a 1% or greater annual chance of flooding). However, due to the unavailability of higher-return-period flood grids, the flood risk of properties located outside the SFHA cannot be quantified. Here, we present a method to estimate flood hazards for U.S. properties that are located both inside and outside the SFHA using existing annual exceedance probability (AEP) surfaces. Flood hazards are characterized by the Gumbel extreme value distribution to project extreme flood event elevations for which an entire area is assumed to be submerged. Spatial interpolation techniques impute flood elevation values and are used to estimate flood hazards for areas outside the SFHA. The proposed method has the potential to improve the assessment of flood risk for properties located both inside and outside the SFHA and therefore to improve the decision-making process regarding flood insurance purchases, mitigation strategies, and long-term planning for enhanced resilience to one of the world's most ubiquitous natural hazards.

1 Introduction

The perilous and expensive nature of flood hazards calls for concurrent improvements in the ability of scientists to measure their risk (Kron 2005). Moreover, rapid increases in the population living in marginal areas relative to the flood hazards (Moulds et al. 2021), amid the consequences of land use changes (Akter et al. 2018; Qiang et al. 2017)), a changing climate (Kreibich et al. 2015; Zhou et al. 2012), sea level rise (Bushra et al. 2021; Nicholls et al. 1999), and local factors such as subsidence (Mostafiz et al. 2021a) and extreme weather events (Guhathakurta et al. 2011), underline the urgent need for accelerated improvements in flood risk assessment (Merz et al. 2014; Mostafiz 2022a). Yet proportionately little advancement has been made. Flood risk maps are often outdated and ignore expression of uncertainty in the depth-duration-return period relationships (Hassini & Guo 2017; Tuyls et al. 2018). Consequences of this gap in scientific analysis ripple into many facets of flood awareness, communication, modeling, planning, preparation, and recovery (Huang & Xiao 2015). Thus, improved quantification of flood hazards, and therefore flood risk, is crucial not only for its own sake, but also for the benefit of other, related efforts to reduce flood-induced losses to life and property (Al Assi et al. 2022; Gnan et al. 2022a; Merz et al. 2014; Mostafiz et al. 2021b, 2022b; Rahim et al. 2022a).

One component of flood hazard quantification that is of particular importance in planning for development is the accurate estimations of return-period-based flood depths (Yang et al. 2020). This is especially important for infrastructure that is expected to be protected during its service over a long period of usefulness (Requena et al. 2013), such as residential and commercial construction, roads, bridges, tunnels, and historical/cultural sites. Not only do lives and livelihoods depend on the protection of such flood-safe infrastructure (Wiering 2019), but renovating and rebuilding these resources after a flood is expensive, disruptive, unpleasant, and incongruent with the ongoing quest for healthier and more resilient individuals and communities (Sayers et al. 2018), if it is possible at all.

Not surprisingly given the paucity of updated scientific work on flood, few if any historical records of such estimates may exist to guide construction, protection, or restoration efforts. Thus, reliance on hydrologic and hydraulic modeling of flood events as a function of annual exceedance probability (AEP; i.e., reciprocal of return period) is necessary (Mostafiz et al. 2021c). However, relatively flood-safe areas often have “null” (i.e., zero or negative) depth values at modeled return periods, even while vulnerability remains substantial during the life span of the infrastructure (Mostafiz et al. 2021c). This leaves even fewer known depth values for planning purposes and may compound flood estimation errors at successively longer return periods, which further weakens efforts to mitigate the impacts of the most destructive floods (Kundzewicz et al. 2013). Therefore, stochastic statistical methods are vital tools to enhance the hydrologic-modeled data for estimating flood (McCuen 2016), to provide construction specialists, architects, developers, and urban and regional planners with adequate information to build more resilient facilities and communities (Olsen et al. 2015).

Previous research has focused on estimating flood hazard and risk for properties located inside the Special Flood Hazard Area (SFHA — areas exposed to 1% or greater annual chance of flooding), where flood insurance is mandatory (e.g., Habete & Ferreira 2017; Johnston & Moeltner 2019; Mobley et al. 2021; Posey & Rogers 2010). The areas outside the SFHA are divided into the “shaded X Zone” (i.e., between 1% and 0.2% annual chance of flooding inundation areas) and the “unshaded X Zone” (i.e., outside of the 0.2% annual chance of flooding inundation area) (Crowell et al. 2010). Generally, no estimates of flood risk exist for properties located in the shaded or unshaded

X Zones (Czajkowski et al. 2013). Additionally, flood insurance is not mandatory in these areas (Kousky 2018), despite the fact that the flood risk is non-zero, may be substantial (especially where valuable and/or expensive infrastructure exists), and may be poorly understood by scientists (Czajkowski et al. 2013). The properties inside the shaded X Zone are considered to have “moderate” flood risk whereas properties inside the unshaded X Zone are labeled as being subjected to “minimal” flood risk (Federal Emergency Management Agency (FEMA) 2005), even though the precise risk throughout the zone is currently unknown. The need for greater quantitative techniques is obvious, so that citizen constituents and government leaders are more aware of the risks that they and their communities face (Mostafiz et al. 2022c, 2021d).

The overarching goal of this research is to characterize flood hazards at locations both inside and outside the SFHA. More specifically, the research addresses the question, “If no modeled flood data exist for some or all return periods, what are the flood characteristics?” To that end, this research introduces a method for describing flood hazards whereby the flood is characterized using the Gumbel extreme value distribution (Nadarajah & Kotz 2004; Waylen & Woo 1982), and flood elevations are projected at higher return periods (Mostafiz et al. 2021c). The gaps in flood surfaces due to limited data are filled by spatial interpolation techniques. These filled elevation values are then used to estimate floods for the locations inside the shaded or unshaded X Zones.

The contribution of this research is the development of a novel method to estimate flood hazard characteristics based on existing modeled flood surfaces. Ultimately, this technique will help government agencies and community officials to formulate policies and homeowners to make more informed decisions regarding insurance purchase (Rahim et al. 2021, 2022b), mitigation strategy (Zarekarizi et al. 2020; Zhou et al. 2012), and long-term planning (Gnan et al. 2022b).

2 Method

The method consists of extrapolating flood depths using the Gumbel extreme value distribution at the locations where a Gumbel fit is possible because flood depths for at least two return periods are known. Extreme return periods are selected where most of the study area is assumed to be submerged (Figure 1). Then, spatial interpolation techniques (Lam 1983), including moving average (e.g., Haining 1978; Chang et al. 1984), inverse distance weighting (IDW; e.g., Fassnacht et al. 2003; Lu & Wong 2008), natural neighbor (e.g., Watson 1999; da Silva et al. 2019), and kriging (e.g., Delhomme 1978; Oliver & Webster 1990), are used to estimate the flood elevation for the extreme return periods at grid cells for which no data-derived distribution can be fit confidently. It is necessary to use flood elevation rather than flood depth for spatial interpolation because flood depth cannot be smoothed across space, while flood elevation is generally insensitive to differences in surface elevation. The imputed extreme-return-period flood elevations are then fit with the Gumbel distribution and used to estimate flood depth for locations that are unflooded at shorter return periods to verify that negative values, confirming that the surface is not flooded at that return period) are returned. Through this method, the flood depth vs. annual non-exceedance probability relationships are established for all locations in the study area, which can then be used to develop flood hazard estimates that are more reasonable to expect within the useful life of the building or settlement.

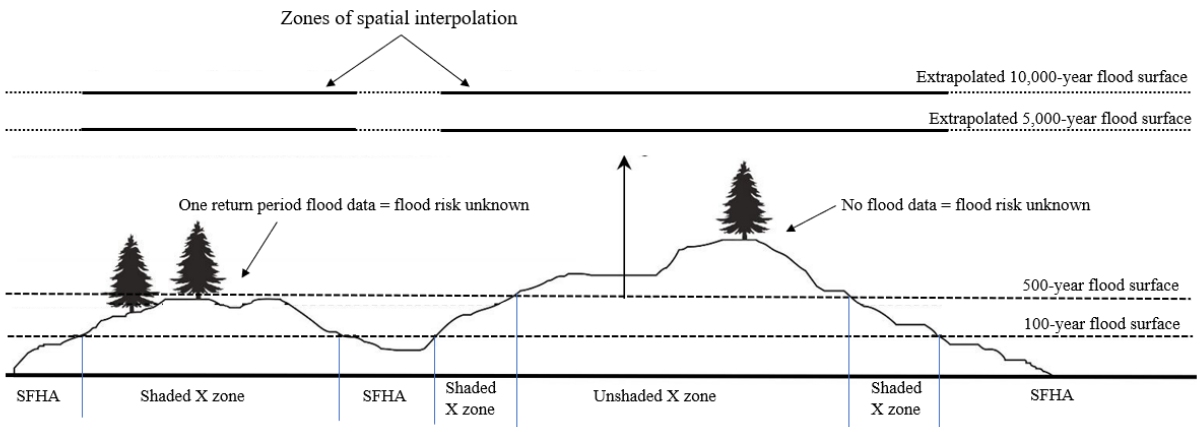


Figure 1. Schematic representation of the concept behind the flood depth surface estimating method.

2.1 Study Area and Data

A frequently-flooded residential neighborhood in Metairie, Louisiana (Jefferson Parish), bounded by the area shown in Figure 2, is used for this case study. This site is chosen primarily because of the availability of model-output flood depth grids for four return periods – 10, 50, 100, and 500 years – developed at a scale of 3.048 m x 3.048 m, by FEMA through its Risk Mapping, Assessment and Planning (Risk MAP) program (FEMA, 2021). The grid cells located within SFHA have at least two flood depth values (i.e., 100- and 500-year return periods) for which the Gumbel distribution can be fit initially (described in Section 2.3). For the grid cells located in shaded-X zone (i.e., only 500-year flood depth is available) or unshaded-X zone (i.e., no flood information available), spatial interpolation is conducted to characterize flood in these grids (described in Section 2.4).

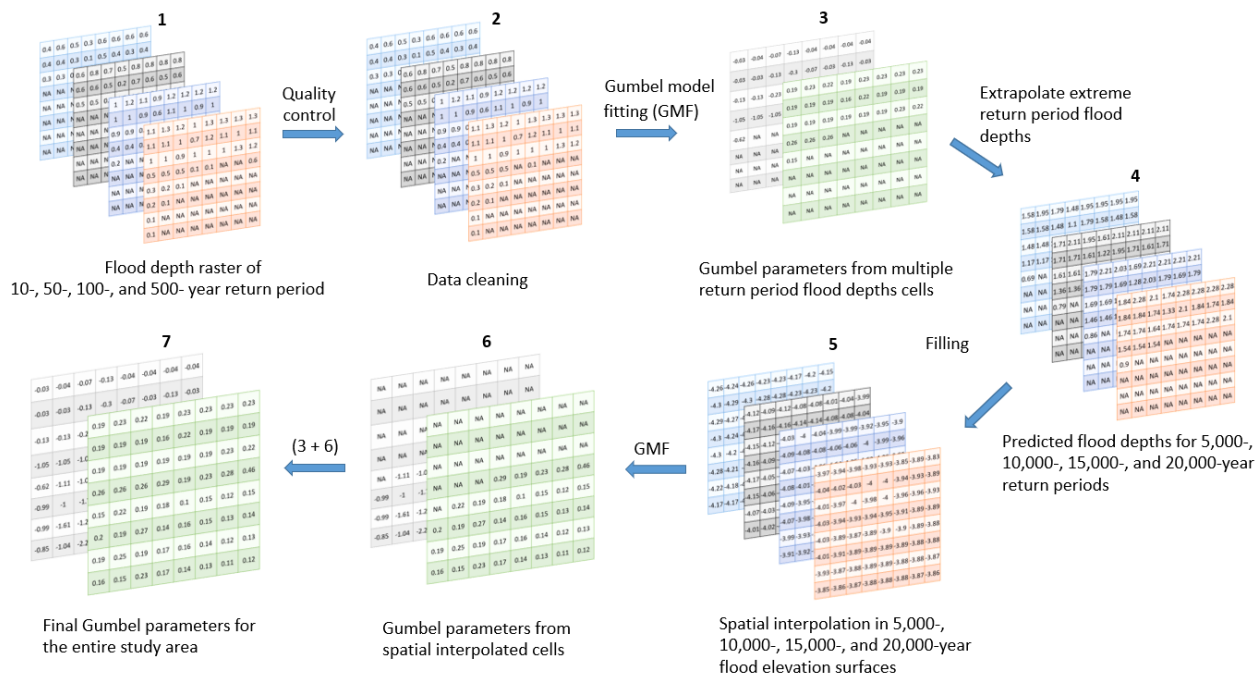
The study area consists of 44 census blocks with a total area of approximately 1.126 km². The mean elevation in this below-sea-level, levee-protected area is -5.5 feet with a standard deviation of 0.71 and a range of -9.0 to -2.9 feet. Descriptive statistics of the Risk MAP-output flood depths by return period are shown in Table 1. The spurious maximum value for the 100-year return period, which is equal to that of the 500-year return period (Table 1), suggests that data cleanup is necessary.



Figure 2. Study area in Metairie, Louisiana.

Table 1. Descriptive statistics of preliminary (uncleaned) flood depths (feet) by return period for the Metairie, Louisiana, study area.

Return Period (years)	Mean (ft.)	Standard Deviation (ft.)	Minimum (ft.)	Maximum (ft.)	Number of Flooded Cells
10	0.67	0.45	0.00	3.40	51,937
50	0.75	0.50	0.00	3.70	68,937
100	0.90	0.58	0.00	4.10	91,163
500	0.93	0.58	0.00	4.10	100,705



140

Figure 3. Schematic summary of the flood hazard characterization method.

2.2 Data Cleaning

Initial quality checks of the source data are performed to identify cells with unrealistic flood depths. The three types of spurious source data are: 1) any cell with a reported flood depth less than or equal to zero for any return period; 2) any cell in which a flood depth for a shorter return period equals or exceeds that for any longer return period; and 3) any cell in which a shorter-duration return period has a reported flood depth but a longer return period has a null (i.e., flood-free) value. Flood depth values for all return periods at any cell that violate any of the three rules above are characterized as “missing.” Flood depth values for cells in which the depth is known (i.e., non-null) for only the 500-year return period are removed here temporarily, but the regression parameters derived are used later to project flood depth as a function of return period for such cells.

2.3 Gumbel Fitting for Cells Flooded by 100-Year Return Period Event

The Gumbel distribution is a widely accepted method for flood frequency analysis (e.g., Kumar & Bhardwaj 2015; Singh et al. 2018). The right-skewed nature of flood return periods makes the Gumbel distribution ideal for estimating the depth vs. annual non-exceedance probability relationship. The two-parameter (i.e., u and α , which are the calculated, site-specific location and scale parameters, respectively) Gumbel extreme value probability density function (PDF) as a function of flood depth (D) is:

$$f(D) = \left(\frac{1}{\alpha}\right) \exp\left\{-\left(\frac{D-u}{\alpha}\right) - \exp\left[-\left(\frac{D-u}{\alpha}\right)\right]\right\} \quad (1)$$

The cumulative distribution function (CDF) is equal to the non-exceedance probability, P , or

$$P = F(D) = \exp\left\{-\exp\left[-\left(\frac{D-u}{\alpha}\right)\right]\right\} \quad (2)$$

Solving for D yields the Gumbel inverse CDF, where D is obtained as a function of P and the Gumbel parameters as:

$$D = F^{-1}[F(D)] = u - \alpha \{\ln[-\ln(P)]\} \quad (3)$$

For each cell having non-null D for at least two return periods, all non-null return periods are used to fit the Gumbel distribution. The site-specific u represents the D at a theoretical, asymptotic approximately-1.58-year return period. Thus, u would be positive for cells located in coastal areas or water bodies and negative for cells located in non-water bodies, including residential areas (Mostafiz et al. 2021c), because a developed area would rarely flood at a 1.58-year return period.

The cells that flood at all four (i.e., 10-, 50-, 100-, and 500-year) return periods are examined first. Such cells that represent a water body are distinguished from those that represent a (flood-prone) terrestrial surface. Each cell that is actually terrestrial and has a negative u is considered to have a plausible Gumbel fit, while each terrestrial cell with a positive u is considered to have a spurious fit. To correct the fit for the cells having a spurious u value, the Gumbel distribution is re-fit while including a “dummy” 2-year return period having a D of -0.05 feet in addition to the known return period depths. A return period of less than two years is cumbersome because calculation of the natural logarithm function for such short return periods yields an unstable result that approaches negative infinity for near-zero return periods. For each cell in which the resulting re-calculated u value based on (now) five return periods then has the appropriate sign, the re-fit Gumbel parameters are accepted. However, for each terrestrial cell in which the re-fit Gumbel distribution again produces a u value with a spurious sign, the iteration of re-fitting the Gumbel distribution (this time using a D of -0.10 feet) is continued, with the process repeated using incremental dummy decreases in D of -0.15 feet, -0.20 feet, etc., with the process ending at the first iteration that generates a negative value for u .

The cells flooded at only three (i.e., 50-, 100-, and 500-year) return periods and having null D (i.e., flood-free) at the shortest (i.e., 10-year) return period are treated next. For such cells, the Gumbel distribution is fit using only the three valid return periods, and D must be estimated for the 10-year return period using the Gumbel distribution with the α and u parameters derived for that cell. If such an estimate yields a negative value for the 10-year return period, the estimation is considered valid. However, if the calculation results in a positive value, correction is necessary because the cell

is known to be flood-free at that return period. In such cases, a dummy 10-year return period D of -0.05 feet is assigned, and the Gumbel distribution is fit once again, this time using this dummy D , along with the output for the three D values for the same cell. For cells in which this new Gumbel fit using the dummy value produces a “correct” condition (i.e., flood-free) regarding D , the revised α and u Gumbel parameters are accepted for that cell. However, for cells in which the “correct” flood condition is still not predicted accurately, the dummy 10-year return period D is replaced by -0.10 feet, and the Gumbel distribution is then run a third time for that cell. For cells in which this new dummy D now generates a “correct” condition, the re-revised α and u parameters are “accepted” for that cell, but for those “null” cells still having a positive calculated 10-year-return-period D , yet another iteration is necessary, this time using a D of -0.15 feet. Each iteration provides more cells with “correct” 10-year-return-period D values, with the α and u Gumbel parameters from the fit that makes the depth “correct” replacing the former parameters. The process continues iteratively, changing the dummy D incrementally by -0.05 feet, until all cells have a “correct” estimation of the 10-year-return-period D .

The cells having known, positive D (i.e., flooded) at only two (i.e., 100- and 500-year) return periods and null D values (i.e., flood-free) at the two shortest (i.e., 10- and 50-year) return periods are treated next. These places are less flood-prone than those analyzed previously. For each of these cells taken individually, the Gumbel α and u parameters are derived based only on the two return periods and are used to estimate the 50-year return-period D . If the calculation results in a positive value, correction is necessary because the cell is known to be flood-free at that return period. In such cases, a dummy 50-year return period D of -0.05 feet is assigned for such cells, and the Gumbel distribution is fit once again, this time using this dummy D , along with the output for the two D values for the same cell. The process continues iteratively, changing the dummy D incrementally by -0.05 feet, until all cells have the “correctly” estimated sign of the 50-year-return-period D . There is no need to repeat the process for the cells that have 10-year-return-period D of the “incorrect” sign, as cells that are not flooded at the 50-year return period will not be flooded at the 10-year return period.

2.4 Parameter Estimation for Cells Not Flooded by 100-Year Return Period Event

At each cell flooded by the 100-year return period event, the unique α and u values are used to extrapolate D at that cell for floods of small probabilities (i.e., higher return periods, including 5,000-, 10,000-, 15,000, and 20,000-year), over which the entire study area is assumed to have flooded. The flood elevation of each of these extrapolated extreme periods is calculated as the sum of D at that return period and the ground elevation of the corresponding cell. It is necessary to use flood elevation rather than D for spatial interpolation because flood elevation is insensitive to differences in surface elevation.

Several spatial interpolation techniques are applied to the study area, separately for each extreme return period (i.e., 5,000-, 10,000-, 15,000, and 20,000-year). A moving average filter is used to impute all missing flood elevation cells in the study area, by experimenting with different window sizes. The dimensions of the final window selected are determined as the smallest that can impute all missing cells, with the same-sized window used for all return periods. Then, because the flood elevation surface of a completely flooded surface should be smooth, a 3x3 moving window is run to smooth the flood elevation surface (i.e., reduce undulations over the flooded terrain). Along with the moving average-smoothing, IDW, natural neighbor, and ordinary kriging spatial interpolation techniques are also used (separately) to impute the missing cell values. Assessment of the relative effectiveness of each technique is conducted. The result of the spatial interpolation

procedure is a complete set of flood elevations at each extreme return period for each cell in the study area, including those cells for which the values were expunged at the shorter return periods.

After deducting the ground elevation, D for the extreme return period events (i.e., 5,000-, 10,000-, 15,000-, and 20,000-year) is used to estimate the flood characteristics in areas unflooded at the 500- and 100-year return periods. Several scenarios are possible. First, for cells that have a positive 500-year D (i.e., are flooded) but are unflooded at 100-year (and shorter) return periods, the Gumbel distribution is fit using the 500-year return period D along with the spatially interpolated estimates at 5,000-, 10,000-, 15,000-, and 20,000-year return periods, and a dummy 100-year return-period D of -0.05 feet. If the resulting estimation of the 100-year return-period D is negative, the values are accepted. However, a (falsely) positive 100-year return period D calculation requires a refitting using the Gumbel distribution for a 100-year return period D of -0.10 feet. Again, if the value is falsely positive, the iteration process continues at incrementally changing dummy values until the 100-year return-period D is (correctly) negative (i.e., null, or flood-free).

A second scenario occurs for cells that have a null D (i.e., unflooded surface) at the 500-year return period but a positive estimated D (i.e., flooded) at the 5,000-year return period. For such cells, the Gumbel distribution is fit using the spatially interpolated estimates at the 5,000-, 10,000-, 15,000-, and 20,000-year return periods along with a dummy D of -0.05 feet for the 500-year return period. The iteration process continues analogously to the previous examples, but with a 500-year return-period D of -0.10 , -0.15 feet, etc. until the 500-year return-period D estimate is (correctly) flood-free.

Likewise, the third scenario involves cells with null (i.e., flood-free) D at 500- and spatially interpolated 5,000-year return periods. In such cases, the Gumbel distribution is fit using the 5,000-, 10,000-, 15,000-, and 20,000-year return period estimates.

The fourth scenario involves correcting any cells for which the spatially interpolated 5,000-year depth is spuriously less than the Risk MAP-modeled 500-year D . In those cases, the Gumbel distribution is fit using the 500-year D along with a dummy flood 100-year return period D of -0.05 feet. If the resulting 100-year value is (falsely) positive, the fitting process continues iteratively (using -0.10 , -0.15 feet, etc.) until the estimated 100-year D becomes a negative value.

2.5 Validation of the Gumbel Fit and Spatial Interpolation Techniques

Model validation is then performed by statistically comparing the estimated D at the 10-, 50-, 100-, and 500-year return periods with the originally available Risk MAP-modeled data. More specifically, the estimated D at the 10-, 50-, 100-, and 500-year return periods should be negative in flood-free cells and positive in flooded cells, as represented in the originally available data. Descriptive statistics are presented based on the estimated and original D values, where the Gumbel distribution is fit initially with the original available D data.

Then, four spatial interpolation methods are implemented (one at a time, separately) to estimate Gumbel parameters (i.e., α and u) for cells having zero or only one non-null D values (i.e., at the 500-year return period), based on values calculated at cells with two or more non-null values. The validity of the Gumbel estimation of D at cells having one non-null value is assessed via the descriptive statistics of the difference between the estimated and Risk MAP-modeled value at the known (i.e., 500-year) return period, by spatial interpolation technique.

2.6 Sensitivity Analysis

A sensitivity analysis is performed, cell by cell, to check the extent to which the success of the estimation procedure, based on the Gumbel parameters, hinges on the number of “known” D values. The model fit is assessed separately via descriptive statistics for the complete set of paired predicted vs. known D values at a particular return period. At each cell, taken one at a time, if D is known from Risk MAP-model-output at 10-, 50-, 100-, and 500-year return periods, the 10-, 50-, and 100-year-return-period D values are used to predict the 500-year-return-period D . An analogous procedure is used for cells that have known D at three return periods. Similarly, the D values at 10- and 50-year return periods are used to predict D at the 100- and 500-year return periods. In each case, the model fit is assessed separately via descriptive statistics of the paired difference between predicted vs. known D .

3 Results

3.1 Data Cleaning

The data cleaning process described in Section 2.2 is run on the 121,215 cells in the study area. Data cleaning identifies 32 cells with D equal to zero (no cells have negative D), 3,575 cells for which a shorter return period D equals or exceeds a longer return period D , and 2,365 cells for which a positive shorter return period D is accompanied by a “null” longer return period D (Table 2). The original D values in these 5,972 cells (4.9% of the initial cells) are thus unused in the analysis because they fail one or more of these data cleaning tests.

Table 2. Number of cells in the study area removed by each data cleaning criterion.

Data Cleaning Rule	Number of Cells
10-year flood depth ≤ 0	13
50-year flood depth ≤ 0	16
100-year flood depth ≤ 0	1
500-year flood depth ≤ 0	2
10-year flood depth \geq 50-year flood depth	776
10-year flood depth \geq 100-year flood depth	0
10-year flood depth \geq 500-year flood depth	2
50-year flood depth \geq 100-year flood depth	530
50-year flood depth \geq 500-year flood depth	4
100-year flood depth \geq 500-year flood depth	2,263
10-year flood depth ≥ 0 and 50-year flood depth is NULL	7
10-year flood depth ≥ 0 and 100-year flood depth is NULL	0
10-year flood depth ≥ 0 and 500-year flood depth is NULL	0
50-year flood depth ≥ 0 and 100-year flood depth is NULL	4
50-year flood depth ≥ 0 and 500-year flood depth is NULL	1
100-year flood depth ≥ 0 and 500-year flood depth is NULL	2,353
Total	5,972

3.2 Gumbel Fitting

Descriptive statistics for the scale (α) and location (u) parameters are shown in Table 3. Once the α and u parameters are corrected for all cells, they are used to extrapolate D for the 5,000-, 10,000-, 15,000-, and 20,000-year return periods in their respective cells.

Table 3. Descriptive statistics of α and u for the location (cells) flooded by more than one return period in the Metairie, Louisiana, study area.

Gumbel Parameter	Mean	Standard Deviation	Minimum	Maximum
α	0.24	0.08	0.08	0.82
u	-0.33	0.37	-3.16	0.00

The smallest possible moving-average window that interpolates all flood elevation values at extreme return periods is 31x31 cells. Descriptive statistics for the spatially interpolated and smoothed Gumbel parameters are shown in Table 4. A negative value is found for u in every cell. The Risk MAP-modeled 500-year D spuriously exceeds the spatially interpolated 5,000-year depth in 36 cells (0.03% of the study area), so correction procedures described in Section 2.4 in the “fourth scenario” are implemented.

Table 4. Descriptive statistics for α and u , after implementing a 31x31 moving average and a 3x3 moving average, based on extrapolated D values of the 5,000-, 10,000-, 15,000-, and 20,000-year return periods, for locations flooded by only one (i.e., 500-year) or no return periods, after removal of spurious cells, for the Metairie, Louisiana, study area.

Gumbel Parameter	Mean	Standard Deviation	Minimum	Maximum
α	0.28	0.22	0.07	2.08
u	-1.72	1.41	-12.96	-0.39

3.3 Validation

The procedure described in Section 2.5 regarding validation of the distribution is implemented for the case study area. Table 5 shows the descriptive statistics and root-mean-square error (RMSE) of the difference between estimated and Risk MAP-modeled data for cells having at least two non-null D values. These results verify that a relatively small amount of error is introduced in the estimation procedure, if it can be assumed that the Risk MAP data are “correct.”

Table 5. Descriptive statistics and root-mean-square error for Risk MAP-modeled minus predicted D , for cells having two or more originally-modeled D from among 10-, 50-, 100-, and 500-year return periods, for Metairie, Louisiana, study area.

	Mean (ft.)	Standard Deviation (ft.)	Minimum (ft.)	Maximum (ft.)	RMSE (ft.)
10-year	0.17	0.21	−0.25	1.58	0.27
50-year	−0.01	0.09	−0.33	0.53	0.09
100-year	0.13	0.07	−0.00	0.85	0.15
500-year	−0.10	0.11	−0.95	0.57	0.14

For cells having only a 500-year Risk MAP-modeled D , the relative correspondence between the spatially interpolated estimated 500-year D and that from Risk MAP is calculated by spatial interpolation technique. Because of the strong correspondence across spatial interpolation methods, values are expressed in inches (Table 6). Results suggest that the selection of spatial interpolation technique has little impact on the results.

Table 6. Descriptive statistics and root-mean-square error for Risk MAP-modeled minus predicted 500-year D , for cells having only 500-year return period flood depth, for the Metairie, Louisiana, study area, by moving average (31x31) and smoothing (3x3), inverse distance weighting, natural neighbor, and ordinary kriging.

Interpolation Technique	Mean (in.)	Standard Deviation (in.)	Minimum (in.)	Maximum (in.)	RMSE (in.)
Moving Average and Smoothing	−1.14	1.30	−11.43	6.90	1.73
Inverse Distance Weighting	−1.12	1.32	−11.43	6.92	1.73
Natural Neighbor	−1.11	1.33	−11.43	6.92	1.73
Ordinary Kriging	−1.12	1.32	−11.43	6.93	1.73

3.4 Sensitivity Analysis

The sensitivity analysis described in Section 2.6 quantifies the rationality of using Gumbel extreme value distribution even as the number of known points decreases to two (Table 7). Results suggest that, not surprisingly, the increased magnitudes of the 500-year D leave a wider range from which the estimate can deviate from the actual D . Also, it is not surprising that the largest standard deviation of this modeled-vs.-estimated difference occurs for predicting the 500-year D when D is known at only two return periods. Nevertheless, even in such cases, the RMSE falls within a half-foot.

Table 7. Descriptive statistics and root-mean-square error of the difference (Δ) between the Gumbel model-based flood depth (D) estimation and Risk MAP-modeled D , when using D at known return periods to predict D at another known return period, for Metairie, Louisiana, study area.

Scenario	Mean (ft.)	Standard Deviation (ft.)	Minimum (ft.)	Maximum (ft.)	RMSE (ft.)
Δ 500-year depth using 10-, 50-, and 100-year depth as predictors	0.32	0.22	-0.26	1.87	0.39
Δ 100-year depth using 10- and 50-year depth as predictors	-0.02	0.20	-0.46	1.09	0.20
Δ 500-year depth using 10- and 50-year depth as predictors	0.28	0.38	-0.46	2.65	0.47

4 Discussion and Limitations

This method offers a means for circumventing the ever-present dilemma of how to ensure high-quality modeling to support planning for preventing, mitigating, and/or adapting to future flood events when little measured data are available, for locations where advanced hydrological and hydraulic modeling has been conducted to determine estimate D at multiple return periods. In the case study area in Metairie, Louisiana, only approximately 5 percent of the cells failed the “data cleaning” tests, which suggests that the modeled data are reasonable. Nearly all of the spurious data occurred when shorter return period D exceeds longer return period D or longer return period D is null.

If it can be assumed that the Risk MAP-modeled data are the “correct” values, the Gumbel distribution-generated flood parameters are shown to be remarkably stable for simulating and imputing D for various return periods. The fact that u remains negative in all cases verifies that the correction algorithm succeeded in ensuring that all terrestrial cells are not submerged under normal conditions. The much smaller standard deviation for α than for u is likely an artifact of the small, homogeneously-elevated study area. As α represents the slope of the Gumbel fit line, each cell in the study area will have a similar relationship between D and P . This contrasts with u , which can have a wider range of values, suggesting that some cells are more susceptible to flooding than others, even within the same neighborhood.

Validation and sensitivity analysis confirm that the method is relatively insensitive to the spatial interpolation technique chosen. The relatively small errors, as evidenced by the small RMSE values (see Table 5), even for 500-year D and even when D values for only two return periods are known, are interpreted as evidence that the procedure is successful. The Gumbel distribution is deemed to provide an acceptable result. Moreover, the relatively small RMSE values, even between estimated vs. modeled 500-year D and even when D values for only two return periods are known,

imply that D can be estimated relatively accurately and precisely. Such estimates can provide engineers and planners with useful information for enhancing infrastructure to accommodate low-frequency, large-magnitude flood events. Although the method is computationally intensive, it can be automated for improved D estimates for any location that is “data rich” regarding D grids at multiple return periods. Refinements in the modeled data for short or long return periods may allow for further improved understanding of infrastructure needs for accommodating floodwaters.

As with any research, there are limitations to the analysis and interpretation of results. Flood hazard estimation is, by necessity, based on such a limited number of data points, but the availability of FEMA-based model output at only a small number of locations and return periods necessitates use of this technique. Moreover, the rounding of original FEMA-modeled values to the tenth of a foot restricts the precision with which the results can be presented. This method was applied to a relatively limited geographical extent with homogeneous topography. Future work should evaluate the performance of the method across a larger geographical extent with more heterogeneous topography. In addition, the effect of climate change on flood hydroclimatology is not considered (Zhou et al. 2012). Changing climate may alter the log-linear shape of the Gumbel distribution, particularly if forecasts of increasing frequency of extreme precipitation events (Intergovernmental Panel on Climate Change 2014, p. 8) prove to be accurate. Likewise, differences in local land cover may cause differences in the Gumbel parameters for D as a function of return period and in generating a continuous surface using the spatial interpolation techniques. Despite the fact that caution should be exercised in the interpretation of results for these and other reasons, the approach offers an advantageous “next step” in planning for, forecasting, and mitigating the world’s most destructive natural hazard.

5 Summary and Conclusions

Existing D grids based on Risk MAP hydrologic and hydraulic model output provide communities with guidance data for anticipating and minimizing flood hazards. However, these depth grids are only available for limited locations and return periods. This study introduces a method for imputing flood depths and elevations for areas considered at low- to moderate-risk, where insufficient flood data are available to characterize the hazard. The method involves fitting the Gumbel extreme value distribution to rasterized flood data of flood depth as a function of annual non-exceedance probability, by cell. The method then uses the Gumbel parameters of scale (α) and location (u) to extrapolate flood elevations at extreme return periods for which it can be assumed that the study area is entirely flooded. Spatial interpolation algorithms are used to fill and smooth spatially the areas that are not flooded by the 100-year flood, and Gumbel scale and location parameters are determined for areas with previously uncharacterized or minimally characterized flood hazards. Validation and sensitivity analyses are conducted through comparison with Risk MAP-modeled output. A case study in Metairie, Louisiana, is used to illustrate the technique. For the study area, different spatial interpolation methods produced similar results when compared to Risk MAP-modeled output D grids. Validation and sensitivity analyses of the case study illustrate that the method offers improvements in characterization of flood hazard for enhanced flood mitigation planning.

Overall, the method performed well across the study area. The specific findings of the case study include that:

- the presented method is able to characterize flood hazards in areas of low to moderate flood risk; for example, 100-year D were predicted for cells with known 100-year D with RMSE of 0.15 feet

- spatial interpolation of extrapolated surfaces functioned well, regardless of technique; for example, 500-year D were imputed using spatial interpolation for cells with known 500-year D with RMSE of 1.73 inches
- using 10-, 50-, and 100-year D as predictors, the estimated 500-year D had an RMSE of 0.39 feet while the estimated 100- and 500-year D had an RMSE of 0.20 and 0.47 feet, respectively, when using 10- and 50-year D as predictors

Future availability of longer-return-period D grids, such as for the 1,000-year flood, will enhance accuracy of our results. Additionally, because many areas have modeled D for only the 100-year return period or for no return periods at all, operationalization of the technique for locations that lack high-quality, modeled D at multiple return periods is needed (Shen et al. 2021). Specifically, ratios between the 100-year D and the D estimated at other return periods, from nearby “data-rich” areas such as Metairie should be calculated as shown here. Then, the ratio between 100-year D and D at other return periods may be used to derive D at other return periods where only the 100-year D has been modeled hydrologically (i.e., “data-medium” areas). Then, the relationship between ground elevation and the 100-year D can be used to identify the 100-year return period D for locations where no hydrological model output is available (i.e., “data poor” areas), based on that from data-rich and data-medium areas. Finally, if such modeling efforts yield plausible results, estimation of D for other return periods in “data-poor” areas can be made based on the Risk MAP output from “data-medium” and “data-rich” areas.

6 Conflict of Interest

The authors declare that the research was conducted in the absence of any commercial or financial relationships that could be construed as a potential conflict of interest.

7 Author Contributions

Mostafiz developed the methodology, collected and analyzed the data, and developed the initial text. Rahim developed the code and helped to develop the methodology. Friedland provided original ideas and advice on the overall project methodology and edited the text. Rohli edited early and late drafts of the text. Bushra expanded the literature review and edited the text. Fatemeh Orooji prepared Figure 1 and helped to validate the code.

8 Funding

This research was funded by the U.S. Department of Homeland Security (Award Number: 2015-ST-061-ND0001-01), the Louisiana Sea Grant College Program (Omnibus cycle 2020–2022; Award Number: NA18OAR4170098; Project Number: R/CH-03), the Gulf Research Program of the National Academies of Sciences, Engineering, and Medicine under the Grant Agreement number: 200010880, “The New First Line of Defense: Building Community Resilience through Residential Risk Disclosure,” and the U.S. Department of Housing and Urban Development (HUD; 2019–2022; Award No. H21679CA, Subaward No. S01227-1). Any opinions, findings, conclusions, and recommendations expressed in this manuscript are those of the authors and do not necessarily reflect the official policy or position of the funders. The publication of this article is subsidized by the LSU Libraries Open Access Author Fund.

9 Reference

- Akter, T., Quevauviller, P., Eisenreich, S. J., & Vaes, G. (2018). Impacts of climate and land use changes on flood risk management for the Schijn River, Belgium. *Environmental Science & Policy*, 89, 163–175. doi: 10.1016/j.envsci.2018.07.002
- Al Assi, A., Mostafiz, R. B., Friedland, C. J., Rahim, M. A., & Rohli, R. V. (2022). Assessing community-level flood risk at the micro-scale by owner/occupant type and first-floor height. In review at *Frontiers in Big Data*. <https://www.essoar.org/doi/abs/10.1002/essoar.10511940.1>
- Bushra N., Mostafiz R. B., Rohli R. V., Friedland C. J., & Rahim M. A. (2021). Technical and social approaches to study shoreline change of Kuakata, Bangladesh. *Frontiers in Marine Science*, 8, Art. No. 730984. doi: 10.3389/fmars.2021.730984
- Chang, T. J., Kavvas, M. L., & Delleur, J. W. (1984). Daily precipitation modeling by discrete autoregressive moving average processes. *Water Resources Research*, 20(5), 565–580. doi: 10.1029/WR020i005p00565
- Crowell, M., Coulton, K., Johnson, C., Westcott, J., Bellomo, D., Edelman, S., & Hirsch, E. (2010). An estimate of the US population living in 100-year coastal flood hazard areas. *Journal of Coastal Research*, 26(2), 201–211. doi: 10.2112/JCOASTRES-D-09-00076.1
- Czajkowski, J., Kunreuther, H., & Michel-Kerjan, E. (2013). Quantifying riverine and storm-surge flood risk by single-family residence: Application to Texas. *Risk Analysis*, 33(12), 2092–2110. doi: 10.1111/risa.12068
- da Silva, A. S. A., Stosic, B., Menezes, R. S. C., & Singh, V. P. (2019). Comparison of interpolation methods for spatial distribution of monthly precipitation in the state of Pernambuco, Brazil. *Journal of Hydrologic Engineering*, 24(3), Art. No. 04018068. doi: 10.1061/(ASCE)HE.1943-5584.0001743
- Delhomme, J. P. (1978). Kriging in the hydrosocieties. *Advances in Water Resources*, 1(5), 251–266. doi: 10.1016/0309-1708(78)90039-8
- Fassnacht, S. R., Dressler, K. A., & Bales, R. C. (2003). Snow water equivalent interpolation for the Colorado River Basin from snow telemetry (SNOTEL) data. *Water Resources Research*, 39(8), Art. No. 1208. doi: 10.1029/2002WR001512
- FEMA. (2005). Flood hazard zones: FEMA coastal flood hazard analysis and mapping guidelines focused study report. Available at: https://www.fema.gov/sites/default/files/2020-03/frm_p1zones.pdf [Accessed August 18, 2022].
- FEMA. (2021). Risk Mapping, Assessment and Planning (Risk MAP). Available at: <https://www.fema.gov/flood-maps/tools-resources/risk-map> [Accessed August 18, 2022].
- Gnan, E., Friedland, C. J., Rahim, M. A., Mostafiz, R. B., Rohli, R. V., Orooji, F., Taghinezhad, A., & McElwee, J. (2022a). Improved building-specific flood risk assessment and implications for depth-damage function selection. *Frontiers in Water*. Art. No. 919726. doi: 10.3389/frwa.2022.919726
- Gnan, E., Friedland, C. J., Mostafiz, R. B., Rahim, M. A., Gentimis, T., Taghinezhad, A., & Rohli, R. V. (2022b). Economically optimizing elevation of new, single-family residences for flood mitigation via life-cycle benefit-cost analysis. *Frontiers in Environmental Science*, 10, Art. No. 889239. doi: 10.3389/fenvs.2022.889239.

- 489 Guhathakurta, P., Sreejith, O. P., & Menon, P. A. (2011). Impact of climate change on extreme
 490 rainfall events and flood risk in India. *Journal of Earth System Science*, 120(3), 359–373. doi:
 491 10.1007/s12040-011-0082-5
- 492 Habete, D., & Ferreira, C. M. (2017). Potential impacts of sea-level rise and land-use change on
 493 special flood hazard areas and associated risks. *Natural Hazards Review*, 18(4), Art. No. 04017017.
 494 doi: 10.1061/(ASCE)NH.1527-6996.0000262
- 495 Haining, R. P. (1978). Moving average model for spatial interaction. *Transactions of the Institute of*
 496 *British Geographers*, 202–225. doi: 10.2307/622202
- 497 Hassini, S., & Guo, Y. (2017). Derived flood frequency distributions considering individual event
 498 hydrograph shapes. *Journal of Hydrology*, 547(2017), 296–308. doi: 10.1016/j.jhydrol.2017.02.003
- 499 Huang, Q., & Xiao, Y. (2015). Geographic situational awareness: mining tweets for disaster
 500 preparedness, emergency response, impact, and recovery. *ISPRS International Journal of Geo-*
 501 *Information*, 4(3), 1549–1568. doi: 10.3390/ijgi4031549
- 502 Intergovernmental Panel on Climate Change. (2014). *Climate Change 2014: Synthesis Report.*
 503 Contribution of Working Groups I, II and III to the Fifth Assessment Report of the Intergovernmental
 504 Panel on Climate Change [Core Writing Team, R.K. Pachauri and L.A. Meyer (eds.)]. IPCC,
 505 Geneva, Switzerland, 151 pp. Available at:
 506 https://www.ipcc.ch/site/assets/uploads/2018/02/SYR_AR5_FINAL_full.pdf [Accessed August 18,
 507 2022].
- 508 Johnston, R. J., & Moeltner, K. (2019). Special flood hazard effects on coastal and interior home
 509 values: one size does not fit all. *Environmental and Resource Economics*, 74(1), 181–210. doi:
 510 10.1007/s10640-018-00314-7
- 511 Kousky, C. (2018). Financing flood losses: A discussion of the National Flood Insurance Program.
 512 *Risk Management and Insurance Review*, 21(1), 11–32. doi: 10.1111/rmir.12090
- 513 Kreibich, H., Bubeck, P., van Vliet, M., & De Moel, H. (2015). A review of damage-reducing
 514 measures to manage fluvial flood risks in a changing climate. *Mitigation and Adaptation Strategies*
 515 *for Global Change*, 20(6), 967–989. doi: 10.1007/s11027-014-9629-5
- 516 Kron, W. (2005). Flood risk= hazard• values• vulnerability. *Water International*, 30(1), 58–68. doi:
 517 10.1080/02508060508691837
- 518 Kumar, R., & Bhardwaj, A. (2015). Probability analysis of return period of daily maximum rainfall
 519 in annual data set of Ludhiana, Punjab. *Indian Journal of Agricultural Research*, 49(2), 160–164.
 520 doi: 10.5958/0976-058X.2015.00023.2
- 521 Kundzewicz, Z. W., Pińskwar, I., & Brakenridge, G. R. (2013). Large floods in Europe, 1985–2009.
 522 *Hydrological Sciences Journal*, 58(1), 1–7. doi: 10.1080/02626667.2012.745082
- 523 Lam, N. S. N. (1983). Spatial interpolation methods: A review. *The American Cartographer*, 10(2),
 524 129–150, doi: 10.1559/152304083783914958
- 525 Lu, G. Y., & Wong, D. W. (2008). An adaptive inverse-distance weighting spatial interpolation
 526 technique. *Computers & Geosciences*, 34(9), 1044–1055. doi: 10.1016/j.cageo.2007.07.010

- 527 McCuen, R. H. (2016). *Modeling Hydrologic Change: Statistical Methods*. CRC press. ISBN: 978-
528 1566706001
- 529 Merz, B., Aerts, J., Arnbjerg-Nielsen, K., Baldi, M., Becker, A., Bichet, A., Blöschl, G., Bouwer, L.
530 M., Brauer, A., Cioffi, F., Delgado, J. M., Gocht, M., Guzzetti, F., Harrigan, S., Hirschboeck, K.,
531 Kilsby, C., Kron, W., Kwon, H.-H., Lall, U., Merz, R., Nissen, K., Salvatti, P., Swierczynski, T.,
532 Ulbrich, U., Viglione, A., Ward, P. J., Weiler, M., Wilhelm, B., & Nied, M. (2014). Floods and
533 climate: emerging perspectives for flood risk assessment and management. *Natural Hazards and*
534 *Earth System Sciences*, 14(7), 1921–1942. doi: 10.5194/nhess-14-1921-2014
- 535 Mobley, W., Sebastian, A., Blessing, R., Highfield, W. E., Stearns, L., & Brody, S. D. (2021).
536 Quantification of continuous flood hazard using random forest classification and flood insurance
537 claims at large spatial scales: a pilot study in southeast Texas. *Natural Hazards and Earth System*
538 *Sciences*, 21(2), 807–822. doi: 10.5194/nhess-21-807-2021
- 539 Mostafiz, R. B., Bushra, N., Rohli, R. V., Friedland, C. J., & Rahim, M. A. (2021a). Present vs.
540 future property losses from a 100-year coastal flood: A case study of Grand Isle, Louisiana. *Frontiers*
541 *in Water*, 3, Art. No. 763358. doi: 10.3389/frwa.2021.763358
- 542 Mostafiz, R. B., Friedland, C. J., Rahman, M. A., Rohli, R. V., Tate, E., Bushra, N., & Taghinezhad,
543 A. (2021b). Comparison of neighborhood-scale, residential property flood-loss assessment
544 methodologies. *Frontiers in Environmental Science*, 9, Art. No. 734294. doi:
545 10.3389/fenvs.2021.734294
- 546 Mostafiz, R. B., Friedland, C. J., Rahim, M. A., Rohli, R. V., & Bushra, N. (2021c). A data-driven,
547 probabilistic, multiple return period method of flood depth estimation. In *American Geophysical*
548 *Union Fall Meeting 2021*. New Orleans, LA, 13–17 December.
549 <https://www.essoar.org/doi/abs/10.1002/essoar.10509337.1>
- 550 Mostafiz, R. B., Bushra, N., Friedland, C. J., & Rohli, R. V. (2021d). Present vs. future losses from a
551 100-year flood: A case study of Grand Isle, Louisiana. In *American Geophysical Union Fall Meeting*
552 *2021*. New Orleans, LA, 13–17 December.
553 <https://www.essoar.org/doi/abs/10.1002/essoar.10509333.1>
- 554 Mostafiz, R. B. (2022a). *Estimation of Economic Risk from Coastal Natural Hazards in Louisiana*.
555 Doctoral Dissertation, Louisiana State University, Baton Rouge, Louisiana. Available at:
556 https://digitalcommons.lsu.edu/gradschool_dissertations/5880
- 557 Mostafiz, R. B., Assi, A. A., Friedland, C. J., Rohli, R. V., & Rahim, M. A. (2022b). A Numerically-
558 integrated approach for residential flood loss estimation at the community level. In *EGU General*
559 *Assembly 2022*. Vienna, Austria, 23–27 May. <https://doi.org/10.5194/egusphere-egu22-10827>
- 560 Mostafiz, R. B., Rohli, R. V., Friedland, C. J., & Lee, Y.- C. (2022c). Actionable information in
561 flood risk communications and the potential for new Web-based tools for long-term planning for
562 individuals and community. *Frontiers in Earth Science*, 10, Art. No. 840250. doi:
563 10.3389/feart.2022.840250
- 564 Moulds, S., Buytaert, W., Templeton, M. R., & Kanu, I. (2021). Modeling the impacts of urban flood
565 risk management on social inequality. *Water Resources Research*, 57(6), Art. No. e2020WR029024.
566 doi: 10.1029/2020WR029024

- 567 Nadarajah, S., & Kotz, S. (2004). The beta Gumbel distribution. *Mathematical Problems in*
568 *Engineering*, 2004(4), 323–332, doi: 10.1155/S1024123X04403068
- 569 Nicholls, R. J., Hoozemans, F. M., & Marchand, M. (1999). Increasing flood risk and wetland losses
570 due to global sea-level rise: Regional and global analyses. *Global Environmental Change*, 9, S69-
571 S87. doi: 10.1016/S0959-3780(99)00019-9
- 572 Oliver, M. A., & Webster, R. (1990). Kriging: A method of interpolation for geographical
573 information systems. *International Journal of Geographical Information Systems*, 4(3), 313–332.
574 doi: 10.1080/02693799008941549
- 575 Olsen, A. S., Zhou, Q., Linde, J. J., & Arnbjerg-Nielsen, K. (2015). Comparing methods of
576 calculating expected annual damage in urban pluvial flood risk assessments. *Water*, 7(1), 255–270,
577 doi: 10.3390/w7010255
- 578 Posey, J., & Rogers, W. H. (2010). The impact of special flood hazard area designation on residential
579 property values. *Public Works Management & Policy*, 15(2), 81–90. doi:
580 10.1177/1087724X10380275
- 581 Qiang, Y., Lam, N. S., Cai, H., & Zou, L. (2017). Changes in exposure to flood hazards in the United
582 States. *Annals of the American Association of Geographers*, 107(6), 1332–1350. doi:
583 10.1080/24694452.2017.1320214
- 584 Rahim, M. A., Friedland, C. J., Rohli, R. V., Bushra, N., & Mostafiz, R. B. (2021). A data-intensive
585 approach to allocating owner vs. NFIP portion of average annual flood losses. In *American*
586 *Geophysical Union Fall Meeting 2021*. New Orleans, LA, 13–17 December.
587 <https://doi.org/10.1002/essoar.10509884.1>
- 588 Rahim, M. A., Gnan, E. S., Friedland, C. J., Mostafiz, R. B., & Rohli, R. V. (2022a). An improved
589 micro scale average annual flood loss implementation approach. In EGU General Assembly 2022.
590 Vienna, Austria, 23–27 May. <https://doi.org/10.5194/egusphere-egu22-10940>
- 591 Rahim, M. A., Friedland, C. J., Mostafiz, R. B., Rohli, R. V., & Bushra, N. (2022b). Apportionment
592 of average annual flood loss between homeowner and insurer. <https://doi.org/10.21203/rs.3.rs-1483728/v1>
- 594 Requena, A. I., Mediero, L., & Garrote, L. (2013). A bivariate return period based on copulas for
595 hydrologic dam design: accounting for reservoir routing in risk estimation. *Hydrology and Earth*
596 *System Sciences*, 17(8), 3023–3038. doi: 10.5194/hess-17-3023-2013
- 597 Sayers, P., Penning-Rowsell, E. C., & Horritt, M. (2018). Flood vulnerability, risk, and social
598 disadvantage: current and future patterns in the UK. *Regional Environmental Change*, 18(2), 339–
599 352. doi: 10.1007/s10113-017-1252-z
- 600 Shen, J., Du, S., Ma, Q., Huang, Q., Wen, J., & Gao, J. (2021). A new multiple return-period
601 framework of flood regulation service—applied in Yangtze River basin. *Ecological Indicators*, 125,
602 Art. No. 107441. doi: 10.1016/j.ecolind.2021.107441

- 603 Singh, P., Sinha, V. S. P., Vijhani, A., & Pahuja, N. (2018). Vulnerability assessment of urban road
604 network from urban flood. *International Journal of Disaster Risk Reduction*, 28(2018), 237–250. doi:
605 10.1016/j.ijdrr.2018.03.017
- 606 Tuyls, D. M., Thorndahl, S., & Rasmussen, M. R. (2018). Return period assessment of urban pluvial
607 floods through modelling of rainfall–flood response. *Journal of Hydroinformatics*, 20(4), 829–845.
608 doi: 10.2166/hydro.2018.133
- 609 Watson, D. (1999). The natural neighbor series manuals and source codes. *Computers &*
610 *Geosciences*, 25(4), 463–466. doi: 10.1016/S0098-3004(98)00150-2
- 611 Waylen, P., & Woo, M.-K. (1982). Prediction of annual floods generated by mixed processes. *Water*
612 *Resources Research*, 18(4), 1283–1286. doi: 10.1029/WR018i004p01283
- 613 Wiering, M. (2019). Understanding Dutch flood-risk management: Principles and pitfalls. In: La
614 Jeunesse, I., & Larrue, C. (Eds.), *Facing Hydrometeorological Extreme Events: A Governance Issue*,
615 Hoboken, NJ: Wiley, pp. 115–124. doi: 10.1002/9781119383567.ch8
- 616 Yang, L., Li, J., Kang, A., Li, S., & Feng, P. (2020). The effect of nonstationarity in rainfall on urban
617 flooding based on coupling SWMM and MIKE21. *Water Resources Management*, 34(4), 1535–1551.
618 doi: 10.1007/s11269-020-02522-7
- 619 Zarekarizi, M., Srikrishnan, V., & Keller, K. (2020). Neglecting uncertainties biases house-elevation
620 decisions to manage riverine flood risks. *Nature Communications*, 11(1), Art. No. 5361. doi:
621 10.1038/s41467-020-19188-9
- 622 Zhou, Q., Mikkelsen, P. S., Halsnæs, K., & Arnbjerg-Nielsen, K. (2012). Framework for economic
623 pluvial flood risk assessment considering climate change effects and adaptation benefits. *Journal of*
624 *Hydrology*, 414(2012), 539–549. doi: 10.1016/j.jhydrol.2011.11.031

625

626 **10 Data Availability Statement**

627 The raw data supporting the conclusions of this article will be made available by the authors, without
628 undue reservation, to any qualified researcher by requesting to the corresponding author.